Direct Measurement of the Rate Constant for the $CH_2(\tilde{X}^3B_1) + CH_3$ Reaction at 300 K

Baoshan Wang† and Christopher Fockenberg*

Brookhaven National Laboratory, Chemistry Department 555A, Upton, New York 11973-5000

Received: April 10, 2001; In Final Form: June 27, 2001

The kinetics of the reaction of ground-state methylene radicals ($\tilde{X}^3B_1$, $^3CH_2$) with methyl radicals (CH_3) has been investigated. Both radicals were produced by the photolysis of acetone ($CH_3C(O)CH_3$) at 193 nm. Using time-resolved time-of-flight mass spectrometry, the temporal evolution of the concentration of reactants as well as products could be observed simultaneously. Rate coefficients at $T = (300 \pm 3)$ K with a bath gas (He) pressure of $P = 133$ Pa (1 Torr) for $^3CH_2 + CH_3$ (1) and $CH_3 + CH_3$ (2) have been determined to be: $k_1 = (2.1 \pm 0.7) \times 10^{-10}$ cm^3 molecule^{-1} s^{-1} and $k_2 = (4.6 \pm 1.0) \times 10^{-11}$ cm^3 molecule^{-1} s^{-1}, respectively.

Introduction

The title reaction has been investigated as part of an effort in our laboratory to study the kinetics and product distribution for the reaction between methyl and hydroxyl radicals, which has two major competing product channels leading either to methanol, CH_3OH, or to singlet methylene ($CH_2(\tilde{a}^1A_1)$, $^1CH_2$) and water.[1] The effects of these competing channels on combustion systems could not be more different. The methanol channel is a chain termination, whereas $^1CH_2$ can react with fuel or hydrogen molecules to maintain the size of the radical pool. To validate theoretical models of the kinetics of this reaction for high pressures and temperatures, for which experimental data are very difficult to obtain, product distributions for low pressures and moderate temperatures ($P \leq 20$ Torr, $T \leq 500$ K) can prove to be very helpful because, under these conditions, the methylene channel can compete effectively with the recombination leading to methanol. In this experiment singlet methylene will mostly be deactivated to triplet methylene, which will further react mainly with the remaining methyl radicals to yield ethylene and hydrogen atoms:

$$^3CH_2 + CH_3 \xrightarrow{k_1} C_2H_4 + H \qquad (1)$$

The concentration−time profile of the transient triplet methylene will, therefore, crucially depend on the rate constant for this reaction.

This reaction has been studied recently at room temperature by Deters et al.[2] using a flow-tube reactor with a microwave discharge as a source for both radicals in combination with Laser Magnetic Resonance (LMR) to detect ground-state methylene radicals. These authors report a rate constant of $k_1 = 1.1 \times 10^{-10}$ cm^3 molecule^{-1} s^{-1} for reaction 1, in agreement with an earlier study by Laufer and Bass[3] who photolyzed mixtures of azomethane and ketene diluted in argon, helium, or nitrogen ($P_{total} = 50-700$ Torr). The product distributions of these systems were measured by gas chromatography and analyzed by fitting the proposed reaction mechanism to the data with k_1 as an adjustable parameter. However, from a similar experiment, Pilling and Robertson[4] deduced a rate constant of just $k_1 = 5 \times 10^{-11}$ cm^3 molecule^{-1} s^{-1}. In a later review article, Laufer[5] pointed out that the predominant difference in the two analyses was the choice of the rate constant for the recombination of methyl radicals:

$$CH_3 + CH_3 \xrightarrow{k_2} C_2H_6 + H \qquad (2)$$

With a currently preferred value for the high-pressure limit of $k_{2,\infty} = 6 \times 10^{-11}$ cm^3 molecule^{-1} s^{-1},[6] both measurements could be brought into agreement leading to an average rate constant of $k_1 = 7 \times 10^{-11}$ cm^3 molecule^{-1} s^{-1}.

Excimer laser photolysis of acetone at $\lambda = 193$ nm was used here as a convenient source for methyl as well as methylene radicals. As pointed out by Lightfoot et al.,[7] a small fraction of the methyl radicals produced undergoes secondary photolysis by the same laser pulse to give methylene radicals and hydrogen atoms. In an earlier investigation in our laboratory on the reaction of methyl radicals with oxygen atoms,[8] we suppressed this process by working at low laser fluences (≤ 30 mJ/cm^2). However, survey studies at higher fluences and acetone concentrations showed a fast decay of methylene radicals that was in conflict with the available literature data on k_1.

The significance of a potentially higher rate constant for reaction 1 to real systems such as flames is that it could increase the buildup of long-chain hydrocarbons in flame fronts via the production of ethylene.[9,10]

In this paper, we report the findings of a detailed study on eq 1 using our time-resolved time-of-flight mass spectrometer (TOF MS) apparatus.

Experimental Section

The experiments were performed using a time-resolved, time-of-flight mass spectrometry apparatus, which has been described in detail elsewhere.[8,11] In brief, the gas mixture composed of precursor molecules as well as bath gas (He, Praxair UHP Grade 5.0, 1−2 Torr) flows through a tubular quartz reactor (10 mm diameter) at a velocity of 13 m/s. Pressure, flow velocity, and the gas mixture are set by mass flow controllers (Tylan General, FC260) in combination with a throttle valve at the end of the reactor. At this flow velocity the maximum observation time is 20 ms, after which dilution with the fresh mixture sets in. A fraction of the gas mixture that escapes from the tube through a pinhole (1 mm diameter) in the wall is photoionized by

* To whom correspondence should be addressed. E-mail: fknberg@bnl.gov.
† E-mail: baoshan@bnl.gov.

10.1021/jp011350q CCC: $20.00
Published on Web 08/17/2001

radiation emitted by a hollow-cathode lamp (McPherson, model 630). The lamp is operated with either Ar ($h\nu = 11.62$ and 11.83 eV) or H_2 (many lines with the main line at 10.2 eV) in the discharge at pressures of 200 mTorr for Ar and 400 mTorr for H_2. The radiation is coupled into the main chamber via a glass capillary in a windowless configuration, which allows the use of the whole emission spectrum of H_2 extending up to 14 eV with an overall intensity at least 10 times higher compared to Ar. Ions are repeatedly extracted into the time-of-flight mass spectrometer (R. M. Jordan Co., D850) by switching voltages at the appropriate grids. Mass spectra are recorded at intervals of 48 μs. Data for one experimental run are acquired by summing signal counts from 100 000 to 200 000 laser shots.

Acetone (Mallinckrodt, 99.7%) as well as 2-butanone (Aldrich, HPLC grade) were degassed by several freeze−pump−thaw cycles and then stored as dilute mixtures in He (Praxair, UHP grade 5.0) in a 20 L glass bulb. For concentration calibrations, additional mixtures of ethane (Linde, >99%), ethylene (Matheson, >99%), carbon monoxide (Matheson, >99%), and 2-butanone in helium were prepared in 3 L glass bulbs. All gases were allowed to mix completely for at least 1 day before use.

To determine the loss of CH_2 radicals in wall reactions, the photolysis of ketene at 193 nm was used as an alternative photolytic source of methylene radicals. Ketene was produced on-line by the pyrolysis of acetic anhydride. For this purpose, helium was bubbled through acetic anhydride, which then passed through an externally heated quartz reactor filled with small quartz pieces. Water and unreacted acetic anhydride were frozen out in a cold trap at dry ice temperature before the ketene/He flow was mixed into the main flow. The drop in the acetic anhydride signal after the oven was turned on showed that more than 90% of the precursor was converted into ketene. Byproducts that could not be frozen out and that entered the reactor were acetone and propanol in concentrations of less than 1% compared to ketene.

For the experimental study on the kinetics of reaction 1 both radicals, CH_3 as well as CH_2, were generated by the 193 nm laser (ArF, Lambda Physik, Compex 205) photolysis of acetone. The primary photolysis pathways are

$$CH_3C(O)CH_3 + h\nu_{193nm} \rightarrow 2\,CH_3 + CO \qquad (3a)$$

with a product yield of $\Phi_{3a} \approx 95\%$[7] and two minor channels leading to

$$\rightarrow CH_2CO + CH_4 \qquad (3b)$$

and

$$\rightarrow CH_3C(O)CH_2 + H \qquad (3c)$$

A fraction of the methyl radicals created by eq 3a was subsequently photolyzed by the same pulse producing methylene (CH_2) radicals:

$$CH_3 + h\nu_{193nm} \rightarrow CH_2 + H \qquad (4)$$

Under our experimental conditions, most of the methylene radicals generated in excited electronic states are rapidly deactivated to the ground electronic state by collisions with bath gas atoms. According to Ashfold et al.[12] the lifetime of singlet methylene is about 10 μs in 1 Torr of helium. Because we discarded data taken in the interval between the laser pulse and 1 ms thereafter (see below), problems arising from reactions of vibrationally hot methyl radicals produced in the 193 nm-photolysis of acetone[13−15] should be minimal because all vibrationally excited methyl radicals should be deactivated on a 100 μs time scale.[16−18] The concentrations of acetone in the reactor ranged from 0.43 to 3.6×10^{13} cm^{-3}. At laser intensities of 35−250 mJ/pulse, of which about 40% could be coupled into the flow tube by collimation with a Galilean telescope, methyl radicals were produced in concentrations of $1.1-9.3 \times 10^{12}$ cm^{-3} yielding methylene-to-methyl ratios ($[CH_2]_0/[CH_3]_0$) between 1/20 and 1/100.

Data Analysis

Reaction Rate. With acetone as the only source for both methyl and methylene radicals the concentration of CH_3 was always in large excess over all other radical concentrations, i.e., mostly methylene radicals and hydrogen atoms: $[CH_2]_0 \approx [H]_0 \leq 4.2 \times 10^{11}$ cm^{-3}. Under these conditions the decay of CH_3 was largely unperturbed by secondary chemistry and, therefore, determined mainly by the self- reaction. In addition, the small absolute concentrations of methylene radicals and hydrogen atoms ensure that the observed kinetics of $^3CH_2$ was primarily governed by the reaction with methyl radicals 1. Although the methylene self-reaction ($k_6 = 5.2 \times 10^{-11}$ cm^3 molecule^{-1} s^{-1})[19] as well as the cross-reaction with hydrogen atoms ($k_5 \approx 2.2 \times 10^{-10}$ cm^3 molecule^{-1} s^{-1})[20,21] are very fast at room temperature, at maximum only 10% of the apparent methylene decay rate would have to be attributed to secondary reactions.

To further establish the error limits made by neglecting secondary reactions, we ran simulation calculations on the following reaction mechanism

$$^3CH_2 + CH_3 \rightarrow C_2H_4 + H \qquad (1)$$

$$CH_3 + CH_3 \rightarrow C_2H_6 \qquad (2)$$

$$CH_2 + H \rightarrow CH + H_2 \qquad (5)$$

$$CH_2 + CH_2 \rightarrow C_2H_2 + H_2 \qquad (6)$$

$$CH_3 + H \rightarrow CH_4 \qquad (7)$$

$$CH + CH_3C(O)CH_3 \rightarrow CH_2 + CH_2C(O)CH_3 \qquad (8a)$$

$$CH + CH_3C(O)CH_3 \rightarrow \text{Products} \qquad (8b)$$

with $k_7 = 1.9 \times 10^{-12}$ cm^3 molecule^{-1} s^{-1} ($P = 1$ Torr of He)[19] and $k_8 = 2.8 \times 10^{-10}$ cm^3 molecule^{-1} s^{-1}, which was assumed to be similar to the reaction of CH + C_2H_6.[19] Because all reactions of CH radicals with hydrocarbons are nearly at their gas kinetic limit, only reactions with acetone were considered. Unfortunately, product distributions of these reactions are not very well-known so that simulations for two limiting cases (either 8a or 8b) were performed. Concentration profiles were calculated with initial concentrations given in experiments number 3 and 10 (see Table 1). To determine the influence of the methyne (CH) chemistry on the methylene profiles, the full mechanism was used with channel 8a open and 8b closed and vice versa, and compared to those obtained by omitting reaction 5. For both experiments, the methylene profiles for reactions 8a open and 5 closed are virtual identical, whereas in the case of reaction 8b open, the time constant for the methylene decay was accelerated by 10% compared to the simulation with reaction 5 closed.

Shutting down reaction 1 had almost no effect on the methyl profile (less than 3% in the rate constant k_2) even if the

TABLE 1: Experimental Conditions and Measured Reaction Rates. Errors in the Reaction Rates are 1σ

expt no.	laser[a] (mJ)	lamp	P (Torr)	$[Acet]_0$ (10^{13}/cm^3)	$[CH_3]_0$ (10^{12}/cm^3)	$[^3CH_2]_0$ (10^{10}/cm^3)	k'_1 (s^{-1})	k'_2 (s^{-1})
1	100	H_2	1.0	1.29	1.79	3.86	480.5 ± 17.0	98.8 ± 1.5
2	100	H_2	1.0	1.92	2.77	3.50	666.4 ± 26.5	142.3 ± 3.9
3	100	H_2	1.0	2.39	3.13	9.22	684.5 ± 19.0	161.6 ± 3.3
4	100	H_2	1.0	3.34	4.66	12.9	1072.1 ± 24.0	223.8 ± 5.7
5	150	H_2	1.0	1.29	2.53	9.49	716.3 ± 19.4	142.7 ± 3.2
6	150	H_2	1.0	2.32	4.60	17.4	1261.7 ± 20.1	230.3 ± 5.0
7	150	H_2	1.0	3.60	6.97	28.3	1806.5 ± 37.1	368.0 ± 11.9
8	210	H_2	1.0	1.29	3.34	11.5	1008.9 ± 24.4	199.4 ± 5.4
9	210	H_2	1.0	2.32	5.86	27.8	1591.2 ± 33.3	319.0 ± 12.2
10	210	H_2	1.0	3.60	9.29	42.4	2710.3 ± 40.4	479.3 ± 20.4
11	35	H_2	1.0	2.86	2.05	0.92	570.2 ± 35.5	86.1 ± 1.0
12	123	Ar	1.0	1.28	2.06	6.15	604.4 ± 23.7	91.1 ± 2.4
13	260	Ar	1.0	0.65	1.93	10.1	638.2 ± 24.3	103.1 ± 5.2
14	260	H_2	1.0	1.41[b]	0.35	0.018	237.3 ± 9.0	37.3 ± 3.0
15	100	H_2	2.0	2.38	3.30	4.69	656.4 ± 23.7	176.5 ± 4.5
16	150	H_2	2.0	1.36	2.70	6.63	558.9 ± 15.1	118.7 ± 1.9
17	210	H_2	2.0	1.36	3.39	9.27	798.2 ± 16.9	151.6 ± 3.3
18	200	H_2	2.0	0.43	1.05	2.64	243.6 ± 15.3	48.1 ± 1.0

[a] Overall pulse energy. [b] CH_3Br as precursor.

methylene radical and hydrogen atom concentrations were as high as 5% of the methyl radical concentration. Because of the continuing generation of hydrogen atoms from reaction 1, approximately 0.5% of the CH_3 radicals were lost in reaction 7 compared to a 95% loss due to the recombination reaction 2 over the calculated interval of 20 ms for experiment 10. Such an additional loss could be modeled by an effective wall reaction rate of about 5 s^{-1}.

In summary, the deviation in the decay time of CH_2 and CH_3 radicals calculated with the full mechanism and the simple reaction scheme involving only reactions 1 and 2 with reaction 2 unperturbed by reaction 1 is expected to be less than 10%, which falls within our experimental error limits. To simplify the analysis, the details of secondary chemistry were neglected. Instead, all secondary reactions were subsumed into estimated first-order loss reactions for the methylene and methyl decays (see below) and treated in the data analysis as effective wall reactions.

In separate experiments using low precursor concentrations (acetone for CH_3 and ketene for CH_2) and low laser intensities we attempted to examine losses of methyl and methylene radicals due to actual wall reactions. In both cases only upper limits for the heterogeneous rate constant of $k_{2w} \leq 10$ s^{-1} for methyl radicals and $k_{1w} \leq 50$ s^{-1} for methylene could be determined because residual self- and cross-reactions could not be separated from the observed decay rate. The high limit for k_{1w} can be explained by the choice of ketene the as CH_2 precursor,[22] which unfortunately does not appear to be a clean photolytic source using 193 nm radiation. We suspect that the coproduction of hydrogen atoms, HCCO, and CCO radicals and their subsequent reactions with methylene radicals gives rise to a linear correlation of the $^3CH_2$ decay time with the laser fluence in the observed intensity range. Because triplet methylene radicals seem to be as reactive as methyl radicals, we assumed that the wall reaction rates of both radicals are identical in our reactor.

Reactions of methylene or methyl radicals with oxygen molecules introduced by impurities in the bath gas or leakage in the vacuum system could be ruled out. The concentration of O_2 in the reactor, which was attributed to the small offset at $m/e = 32$, was determined to be less than 5×10^{10} cm^{-3} for all experiments. At these low O_2 concentrations in combination with the small radical concentrations used here, rates for $CH_2 + O_2$ and $CH_3 + O_2$ reactions were less than 1 s^{-1} and, therefore, negligible.

Including wall reactions, the observed CH_3 and $^3CH_2$ concentration profiles can be described analytically as follows[23,24]

$$\frac{[CH_3]_t}{[CH_3]_0} = \exp(-k_{2w}(t - t_0)) \times \left[\frac{k_{2w}}{2k_2[CH_3]_0(1 - \exp(-k_{2w}(t - t_0)) + k_{2w}}\right] \quad \text{(Ia)}$$

$$\frac{[^3CH_2]_t}{[^3CH_2]_0} = \exp(-k_{1w}(t - t_0)) \times \left[\frac{k_{2w}}{2k_2[CH_3]_0(1 - \exp(-k_{2w}(t - t_0)) + k_{2w}}\right]^{k_1/2k_2} \quad \text{(IIa)}$$

In the limit of $k_{2w} \rightarrow 0$ (no wall reactions) we, of course, get the simple expression for a second-order self-reaction of methyl radicals

$$\frac{[CH_3]_t}{[CH_3]_0} = \frac{1}{2k_2[CH_3]_0(t - t_0) + 1} \quad \text{(Ib)}$$

Comparing equations (Ia) and (IIa) leads to a different form for the $^3CH_2$ decay profile:

$$\frac{[^3CH_2]_t}{[^3CH_2]_0} = \exp\left[-\left(k_{1w} - \frac{k_1}{2k_2}k_{2w}\right)(t - t_0)\right] \times \left(\frac{[CH_3]_t}{[CH_3]_0}\right)^{k_1/2k_2} \quad \text{(IIb)}$$

Keeping in mind that the methyl radical chemistry is assumed to be decoupled from reactions involving methylene radicals, and that the methylene kinetics mainly depends on reactions with methyl radicals, this leads to the following strategy for analyzing the experimental data: First, eq Ia was fit to the methyl profile with $[CH_3]_0$ and $k'_2 = k_2[CH_3]_0$ as fit parameters. Then the methylene decay was fitted by taking the obtained fit curve for the methyl profile, inserting it into eq IIb, and varying $[^3CH_2]_0$ and the ratio $r_{12} = k_1/2k_2$. Finally the decay rate k'_2 for the methyl self-reaction was plotted against the methyl radical concentration giving the rate constant k_2, which was then used to calculate k_1 from r_{12}.

Concentration of Methyl Radicals. The concentration of methyl radicals was calculated for each experiment directly from

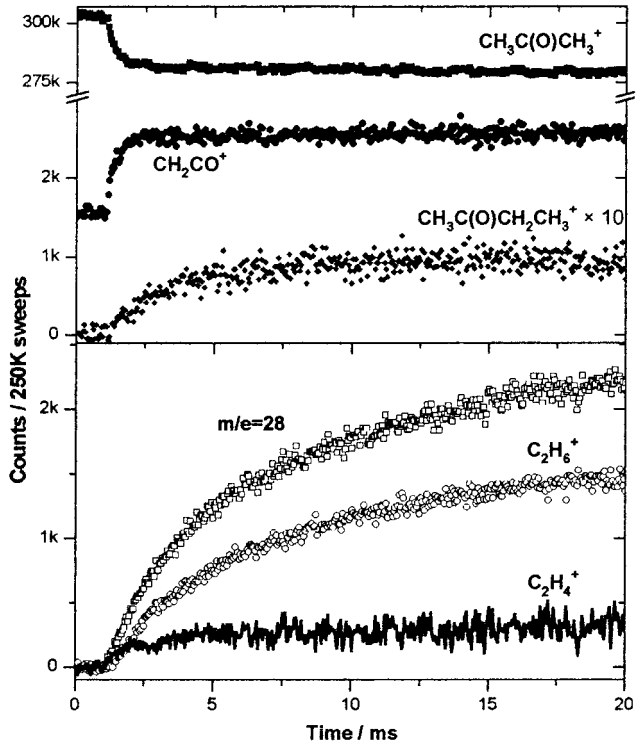

Figure 1. Ion signals plotted vs time for several species acquired in experiment #1 (see Table 1). The solid line in the lower panel shows the net counts of C_2H_4 produced in the reaction of $^3CH_2$ with CH_3 after subtracting the contributions from the cracking of C_2H_6 and CO.

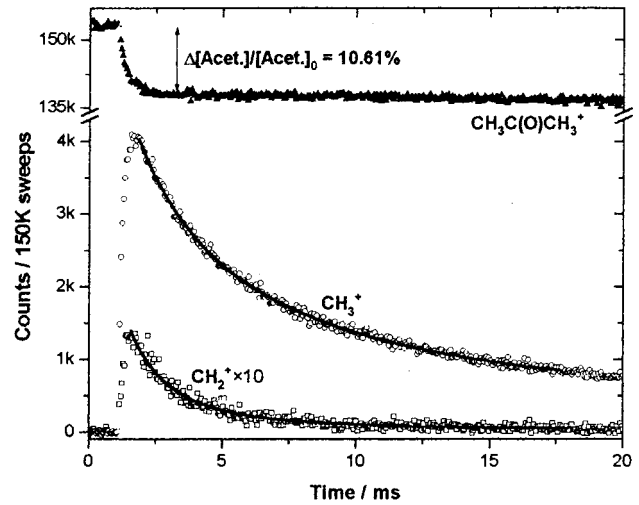

Figure 2. Ion signals associated with CH_3, $^3CH_2$, and acetone plotted vs time acquired in experiment #5 (see Table 1). The solid lines are fits of expressions (Ia) and (IIb) to the data.

the relative drop, *R*%, of the acetone ion signal at $m/e = 58$ after the laser fired (see Figures 1 and 2):

$$R\% = \frac{\Delta\{\text{Acet.}^+\}}{\{\text{Acet.}^+\}_{before}} \times 100\% = \frac{\{\text{Acet.}^+\}_{\text{before}} - \{\text{Acet.}^+\}_{after}}{\{\text{Acet.}^+\}_{before}} \times 100\% \quad \text{(III)}$$

The braces {..} are used to indicate actual, experimental signal counts of the species in question. As mentioned above, there are two additional, minor channels, (3b) and (3c), in the photolysis of acetone. The product yield of channel (3b) leading to ketene, Φ_{3b}, which could clearly be observed at $m/e = 42$ (see Figure 1), was determined by measuring the net increase of ketene in reference to the drop in acetone. For this purpose, we introduced calibration ratios, *CR*, which are ratios of individual calibration constants, in this case for absolute ketene and acetone concentrations. Calibration constants were obtained in separate experiments. With $CR(CH_2CO, 42:\ \text{Acetone}, 58) = 2.25 \pm 0.50$ the ketene yield could be calculated via

$$\Phi_{3b} = \left\{ \frac{\Delta\{\text{Ketene}^+\}}{\Delta\{\text{Acetone}^+\}} / CR(\text{Ketene, 42:Acetone, 58}) \right\} \quad \text{(IV)}$$

As an average value over all measurements we obtained $\Phi_{3b} = (2.2 \pm 0.5)\%$, which is in good agreement with the upper limit of 2% given by Lightfoot et al.[7] For channel 3c it was unfortunately not possible to distinguish between acetonyl radicals, $CH_3C(O)CH_2$, at $m/e = 57$ generated in the photolysis of acetone from those created as fragments in the photoionization of acetone. An alternate method to estimate the branching ratio for channel 3c is to employ the signal at $m/e = 72$, which we attributed as methyl ethyl ketone (MEK, 2-butanone) produced in the reaction of acetonyl with methyl radicals:

$$CH_3C(O)CH_2 + CH_3 \xrightarrow{k_9} CH_3C(O)CH_2CH_3 \qquad (9)$$

Using the same analysis as for reaction 1 and assuming that all acetonyl radicals react only with methyl according to reaction 9, we calculate a yield of $\Phi_{3c} = (0.5 \pm 0.2)\%$ with $CR(\text{MEK}, 72:\ \text{Acetone}, 58) = 1.47 \pm 0.02$. This result is significantly smaller than the estimate of 3% reported by Lightfoot et al.[7] However, there are three potential problems associated with our determination: First, reaction 9 might not be the only product channel, which would explain the lower yield. Second, acetonyl might be lost in other reactions with the same result as above. Third, MEK might be produced via an insertion of singlet methylene into a C−H bond of acetone. However, the rates of similar $^1CH_2$ insertions into the C−H bonds of comparable hydrocarbons[5] are only as fast as the deactivation to triplet methylene in collision with bath gas molecules implying that only a small fraction (<1% of all generated singlet methylene radicals) could theoretically react with acetone to give MEK. Considering the various uncertainties, we chose a value of $\Phi_{3a} = 96\%$ as primary product yield for channel (3a).

Because methyl radicals act as precursors for methylene radicals, the photolytic loss of CH_3 has to be accounted for in order to get a more accurate value for $[CH_3]_0$. A direct measurement of the absolute initial concentration of $^3CH_2$ is difficult. Instead we used the fact that ethylene, C_2H_4, is the dominant product channel of reaction 1[5] to calibrate $^3CH_2$ by setting $[C_2H_4]_{t\to\infty}$ equal to $[^3CH_2]_0$. Besides C_2H_4, the signal at $m/e = 28$ also includes contributions from the cracking of C_2H_6 and to a minor extent from CO generated in the photolysis of acetone. All of these contributions can be accounted for through appropriate calibration constants. A typical net counts-versus-time profile after corrections is shown as the solid line in Figure 1. Now the absolute concentration of $[^3CH_2]_0$ can be calculated as follows

$$[^3CH_2]_0 = [C_2H_4]_{t\to\infty} = \frac{\Delta\{C_2H_4^+\}}{CR(C_2H_4, 28:\text{Acet.}, 58) \times \Delta\{\text{Acet.}^+\}} \times [\text{Acet.}]_0 \times R\% \quad \text{(V)}$$

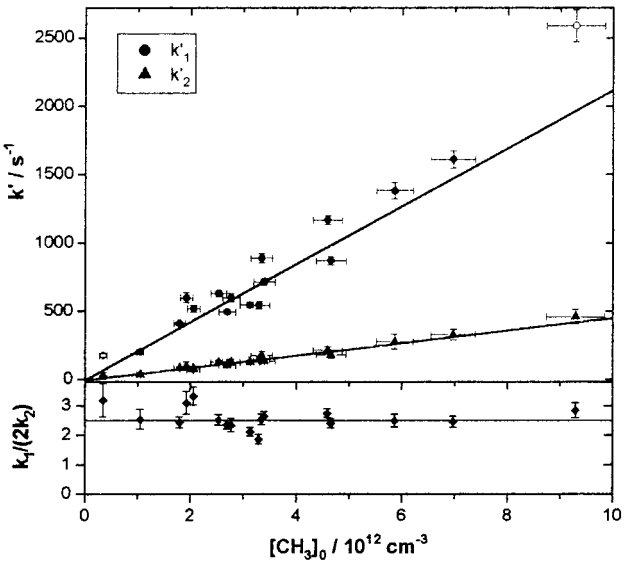

Figure 3. Second-order plots for reaction rate from the decay of methyl and methylene radicals (upper panel). For k'_1 the points indicated by hollow circles were excluded in the fit. The $r_{12} = k_1/2k_2$ ratios are shown in the lower panel. The line indicates the average value with $r_{12,avg} = 2.5 \pm 0.2$.

Finally, the initial concentration of CH_3 was calculated via

$$[CH_3]_0 = 2 \times \Phi_{3a} \times [\text{Acet.}]_0 \times R\% - [^3CH_2]_0 \quad \text{(VI)}$$

The resulting absolute initial concentrations of $^3CH_2$ and CH_3 are listed in Table 1.

Methyl Recombination Rate. The methyl concentration profile was fitted according to expression (Ia) for three different wall reaction rates $k_{2w} = 0$, 10 s^{-1}, or 20 s^{-1}. The resulting reaction rates, $k'_2 = k_2[CH_3]_0$, were then plotted against the methyl radical concentrations, from which the final rate constant could be obtained through a linear least-squares fit (see Table 1 and Figures 2 and 3). The observable rise or decay in the concentration profiles after the photolysis pulse is caused by the finite travel time from the orifice in the reactor wall to the ionization region. To avoid any influence of this effect on the fit we used only those data points that were recorded after 1 ms following the firing of the laser. For $k_{2w} = 0$ and 10 s^{-1} the fits were indistinguishable giving rate constants of $k_2(k_{2w} = 0) = (5.2 \pm 0.5) \times 10^{-11}$ cm^3 $molecule^{-1}$ s^{-1} and $k_2(k_{2w} = 10\ s^{-1}) = (4.6 \pm 0.3) \times 10^{-11}$ cm^3 $molecule^{-1}$ s^{-1} with intercepts close to the origin. Uncertainties are given as 2σ (statistical error). As anticipated, higher values for the wall reaction rates deteriorate the quality of the fit significantly in particular at longer times ($t \geq 15$ ms) and were, therefore, neglected. In view of the assumptions made and uncertainties regarding heterogeneous and disregarded radical−radical reactions, we prefer to present $k_2(k_{2w} = 10\ s^{-1})$ as the final methyl−methyl recombination rate constant at $T = (300 \pm 3)$ K and $P = 1$ Torr (He):

$$k_2 = (4.6 \pm 1.0) \times 10^{-11}\ \text{cm}^3\ \text{molecule}^{-1}\ \text{s}^{-1}.$$

We chose a larger error instead of the pure statistical error reflecting the apparent uncertainties in particular with respect to the quantification of the methyl radical concentration, which we estimated to be accurate to about 10%. However, we do not expect the true value to lie outside of the quoted error limit.

Methyl−Methylene Reaction Rate. With the predetermined methyl profile for each measurement, we fit expression (IIb) to the $^3CH_2$ data with the term $k_{1w} - r_{12} \times k_{2w}$ set to zero (see Figure 2). The obtained ratios $r_{12} = k_1/2k_2$ are plotted in the lower part of Figure 3. Averaging the ratios gives a value of $r_{12,avg} = 2.5 \pm 0.2$ (2σ), from which a rate constant for reaction 1 can be derived to be $k_1(r_{12,avg}) = (2.3 \pm 0.6) \times 10^{-10}$ cm^3 $molecule^{-1}$ s^{-1} using $k_2 = (4.6 \pm 1.0) \times 10^{-11}$ cm^3 $molecule^{-1}$ s^{-1}. Alternatively, the reaction rates for reaction 1, k'_1, can be calculated from the methyl radical recombination rates, $k'_1 = r_{12} \times k'_2$, and plotted against $[CH_3]_0$ (see Table 1 and Figure 3). Because the linear fit offers one additional fit parameter (intercept) compared to the simple average, the rate constant differs slightly from the above value. In addition, the reaction rate at the highest methyl radical concentration was treated as an outlier. Its obvious deviation from the fitted line was probably caused by effects due to secondary reactions. From the slope, the second-order rate constant for reaction 1 was determined to be:

$$k_1 = (2.1 \pm 0.7) \times 10^{-10}\ \text{cm}^3\ \text{molecule}^{-1}\ \text{s}^{-1}$$

at $T = (300 \pm 3)$ K and $P = 1$ Torr (He). Even though the exponential term in eq IIb was neglected, its influence on the methylene fit is only marginal due to cancellation effects in the term: $k_{1w} - r_{12} \times k_{2w}$. However, the error given here again reflects the uncertainties as mentioned for k_2 and indicated in the simulation results. Using the rate constants obtained from the second-order plot gives a slightly lower value for the ratio, r_{12}, than the average value: $r_{12,fit} = 2.3 \pm 0.2$ (2σ).

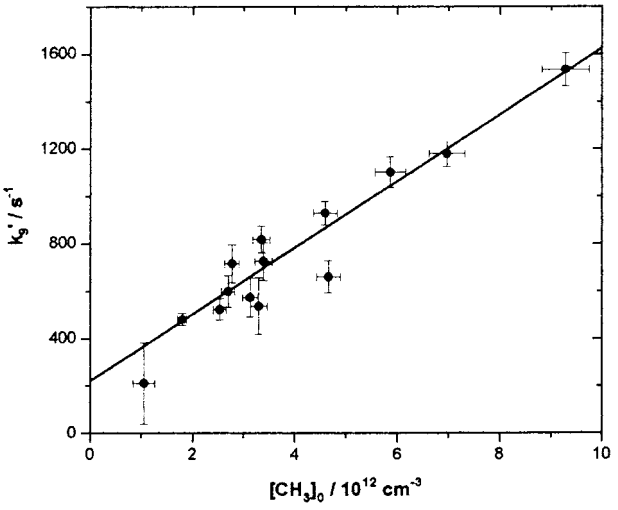

Figure 4. Second-order plot for reaction rate k'_9 from the analysis of the signal at $m/e = 72$.

Methyl-Acetonyl Reaction Rate. For completeness, the signal at $m/e = 72$, which we attributed to originate from reaction 5, was analyzed following the same kinetic analysis used for reaction 1. The plot of $k'_9 = k_9[CH_3]_0$ is shown in Figure 4. From the slope the rate constant was determined to be

$$k_9 \leq 1.4 \times 10^{-10}\ \text{cm}^3\ \text{molecule}^{-1}\ \text{s}^{-1}$$

It should be noted that the signal-to-noise ratio for the $m/e = 72$ channel is relatively low due to the small concentration of MEK. In addition, this mass channel might also include contributions from other reactions (see above). Therefore, we consider k_9 as an upper limit for the rate constant for reaction 9.

Discussion

In the present study, we have measured the rate constants for the reaction of methyl with methylene radicals, k_1, and the

TABLE 2: Rate Constants for the Methylene-methyl Cross Reaction and the Methyl−Methyl Recombination Reaction

reaction	T/K	bath gas and pressure/Torr	$k/10^{-11}$ cm^3 s^{-1}	ref
$CH_2 + CH_3$	300	He, 1.0	21 ± 7	this work
	300	Ar, He, N_2, 50−700	10	Laufer & Bass[3]
	300	Ar, 200	5	Pilling & Robertson[4]
	300	He, 1.0	11, 17[a]	Deters et al.[2]
$CH_3 + CH_3$	300	He, 1.0	4.6 ± 1.0	this work
	307	He, 1.0	4.1	Stoliarov et al.[24]
	298	He, 1.0	2.5	Cody et al.[25]
	300	He, 1.0	2.9	Deters et al.[2]
	296	Ar, 1.0	5.3[b]	Hessler & Ogren[29]
	290	He, 7.8−667	5.2[c]	De Avillez Pereira et al.[1]
	300	Ar, 1.0	3.5[d]	Baulch et al.[6]
	296	Ar, 2.8	4.4[e]	Slagle et al.[30]
		Ar, 4.0	5.1[f]	
		He, 3.9	3.6[e]	
	298	He, 5−700	9.53	Laufer & Bass[3]

[a] Calculated from their $k_1/2k_2 = 1.9$ and our $k_2 = 4.6 \times 10^{-11}$ cm^3/s. [b] Calculated from "J-equation" global fit. [c] Average value. [d] Calculated from recommended values k^0, k^∞, and F_c. [e] Mass spectroscopy experiment [f] UV-absorption experiment

recombination of two methyl radicals, k_2, simultaneously by observing both radicals directly. Literature data on both rate constants for room temperature and, in particular for k_2, at low pressures can be seen in Table 2. Our value for k_1 is about twice as high as the rate constant reported by Deters et al.[2] obtained under essentially the same temperature, pressure, and radical concentration conditions and more than three times as large as Laufer and Pilling's corrected value measured at higher pressures.[5] Interestingly, the main difference between Deters' results and ours lies in the rate constant for the methyl recombination, for which these authors obtained an average value of $k_2 = 2.9 \times 10^{-11}$ cm^3 molecule^{-1} s^{-1}. Because their data analysis essentially is the same as ours, we should not compare rate constants but their ratio, r_{12}, instead. Indeed, we calculate a value of $r_{12,avg} = k_1/2k_2 = 1.9 \pm 0.2$ from their rate constants, which is only about 25% lower than the ratio found in this work ($r_{12,avg} = 2.5 \pm 0.2$). Therefore, applying our result for k_2 would raise Deters' rate constant for reaction 1 to 1.7×10^{-10} cm^3 molecule^{-1} s^{-1}.

In fact, very recently, Stoliarov et al.[24] reported a rate constant of $k_2 = 4.1 \times 10^{-11}$ cm^3 molecule^{-1} s^{-1} at $T = (307 \pm 4)$ K and 1 Torr of He using an experimental apparatus similar to ours. The discrepancy between the methyl radical recombination rate constant found here and Stoliarov's can be explained by the fact that these authors set the zero-time point, t_0, at the time when the methyl radical signal reached the half of its maximum value, which usually meant a delay between laser pulse and t_0 of about 0.2 ms. Because their experimental setup and ours are comparable, we think that the finite rise time in the radical signal is caused by the finite time any species needed to reach the ionization region and establish a steady-state flux. However, the chemistry is already progressing in the time interval since the laser fired. In a separate analysis of our data applying the same t_0-shift used by Stoliarov et al. we arrived at the same lower rate constant, k_2. In any case, this indicates that the recombination rate constant, k_2, at room temperature and 1 Torr helium is indeed higher than the one given by Deters et al.

In contrast to Stoliarov's and our results, Cody et al.[25] measured the methyl−methyl recombination rate constant with a discharge-flow reactor apparatus and reported a value of $k_2 = 2.5 \times 10^{-11}$ cm^3 molecule^{-1} s^{-1} at $T = 298$ K and 1 Torr (He) seemingly confirming Deters' rate constant. Both groups were using essentially the same method for the generation of methyl radicals but with different analytical techniques (quadrupole mass spectrometer vs LMR). The only fundamental difference between these four measurements seems to be the method of creating radicals and determining their concentration, i.e., discharge and conversion/titration vs photolysis and observation of the precursor species. To resolve this problem an independent measurement for methyl radicals is probably needed.

Laufer and Pilling's experiments are conceptually very different than ours. The rate constants were obtained from fitting a complex reaction mechanism to product yields in a system containing relatively high and comparable concentrations of methyl and methylene radicals as well as hydrogen atoms. The quality of fitting such a system depends crucially on the completeness of the reaction mechanism. We suspect that the addition of the fast reaction 5, $CH_2 + H \rightarrow H_2 + CH$, which had been left out originally, might play a significant role in this respect. To test this idea, we added this reaction to Laufer and Pilling's reaction mechanism and calculated the net flux into methyne radicals for Laufer and Bass's 200 Torr Ar case. We estimated the initial radical concentrations from the product distributions of the separate azomethane- and ketene-photolysis experiments. Although the initial hydrogen atom concentration was about 15 and 35 times lower compared to the methyl and methylene concentration, the final CH concentration was about the same as for C_2H_2, C_2H_4, and 2.5 times higher than the final C_2H_6 concentration. The exact influence of adding further methyne reactions to the mechanism on the measured product yields is difficult to predict in particular because data on kinetics and product distributions of CH reactions in particular with the precursor molecules used (azomethane and ketene) is almost completely unknown.

One potential source of error in our experiment was the use of hydrogen as discharge medium in the hollow cathode lamp. Although the ionization of carbon monoxide (ionization potential = 14.01 eV)[26] should have been highly unlikely, we could clearly detect CO with an efficiency about 200 times less compared to acetone. This gives rise to the assumption that a fraction of the methyl radicals might fragment into methylene ions (appearance potential = 15.09 eV)[27] after photoionization. To validate this assumption we used an Ar discharge instead of H_2, eliminating the problem of high-energy photons. However, the kinetics of either methyl or methylene radicals were not altered so that fragmentation could be safely disregarded.

Conclusion

To the best of our knowledge, the rate constant for the $^3CH_2 + CH_3$ reaction, k_1, used in all combustion-simulation-related

reaction mechanisms is based on Laufer's reevaluation. In contrast to this number, we found a considerably higher value, suggesting that this rate constant should be reconsidered. However, the implication for combustion systems can only be ascertained in an actual combustion simulation, which lies outside the scope of our research program. The main problem in the analysis of k_1 appears to be the correct rate constant for the methyl radical recombination, k_2, which still is controversial at pressures around 1 Torr with helium as a collision partner. Experiments at higher pressures in argon can be useful for resolving this problem because the large body of available experimental and theoretical data[28,29] for these conditions appears to be in better agreement with each other.

Acknowledgment. This work was performed at Brookhaven National Laboratory under Contract No. DE-AC02-98CH10886 with the U.S. Department of Energy and supported by its Division of Chemical Sciences, Office of Basic Energy Sciences.

References and Notes

(1) De Avillez Pereira, R.; Baulch, D. L.; Pilling, M. J.; Robertson, S. H.; Zeng, G. *J. Phys. Chem. A* **1997**, *101*, 9681.
(2) Deters, R.; Otting, M.; Wagner, H. G.; Temps, F.; Dóbé, S. *Ber. Bunsen-Ges. Phys. Chem.* **1998**, *102*, 978.
(3) Laufer, A. H.; Bass, A. M. *J. Phys. Chem.* **1975**, *79*, 1635.
(4) Pilling, M. J.; Robertson, J. A. *Chem. Phys. Lett.* **1975**, *33*, 336.
(5) Laufer, A. H. *Rev. Chem. Intermed.* **1981**, *4*, 225.
(6) Baulch, D. L.; Cobos, C. J.; Cox, R. A.; Frank, P.; Hayman, G.; Just, T.; Kerr, J. A.; Murrels, T.; Pilling, M. J.; Troe, J.; Walker, R. W.; Warnatz, J. *J. Phys. Chem. Ref. Data* **1994**, *23*, 847.
(7) Lightfoot, P. D.; Kirwan, S. P.; Pilling, M. J. *J. Phys. Chem.* **1988**, *92*, 4938.
(8) Fockenberg, C.; Hall, G. E.; Preses, J. M.; Sears, T. J.; Muckerman, J. T. *J. Phys. Chem. A* **1999**, *103*, 5722
(9) Leung, K. M.; Lindstedt, R. P. *Comb. Flame* **1995**, *102*, 129.
(10) Wang, H.; Frenklach, M. *Comb. Flame* **1997**, *110*, 173.
(11) Fockenberg, C.; Bernstein, H. J.; Hall, G. E.; Muckerman, J. T.; Preses, J. M.; Sears, T. J.; Weston, R. E., Jr. *Rev. Sci. Instrum.* **1999**, *70*, 3259.
(12) Ashfold, M. N. R.; Fullstone, M. A.; Hancock, G.; Ketley, G. W. *Chem. Phys.* **1981**, *55*, 245.
(13) Donaldson, D. J.; Leone, S. R. *J. Chem. Phys.* **1986**, *85*, 817.
(14) Hall, G. E.; Vanden Bouten, D.; Sears, T. J. *J. Chem. Phys.* **1991**, *94*, 4182.
(15) North, S. W.; Blank, D. A.; Gezelter, J. D.; Longfellow, C. A.; Lee, Y. T. *J. Chem. Phys.* **1995**, *102*, 4447.
(16) Callear, A. B.; Van den Bergh, H. E. *Chem. Phys. Lett.* **1970**, *5*, 23.
(17) Donaldson, D. J.; Leone, S. R. *J. Phys. Chem.* **1987**, *91*, 3128.
(18) Rudolph, R. N.; Hall, G. E.; Sears, T. J. *J. Chem. Phys.* **1996**, *105*, 7889.
(19) Baulch, D. L.; Cobos, C. J.; Cox, R. A.; Esser, C.; Frank, P.; Just, T.; Kerr, J. A.; Pilling, M. J.; Troe, J.; Walker, R. W.; Warnatz, J. *J. Phys. Chem. Ref. Data* **1992**, *21*, 411.
(20) Fulle, D.; Hippler, H. *J. Chem. Phys.* **1997**, *106*, 8691.
(21) Rohrig, M.; Petersen, E. L.; Davidson, D. F.; Hanson, R. K.; Bowman, C. T. *J. Chem. Phys. A* **1997**, *106*, 8691.
(22) Glass, G. P.; Kumaran, S. S.; Michael, J. V. *J. Phys. Chem. A* **2000**, *104*, 8360.
(23) Niiranen, J. T.; Gutman, D. *J. Phys. Chem.* **1993**, *97*, 9392.
(24) Stoliarov, S. I.; Knyazev, V. D.; Slagle, I. R. *J. Phys. Chem. A* **2000**, *104*, 9687.
(25) Cody, R. J.; Payne, W. A.; Thorn, R. P.; Stief, L. J.; Nesbitt, F. L.; Iannone, M. A. *American Astronomical Society* **2000**, *DPS meeting #32*, #15.02.
(26) Erman, P.; Karawajczyk, A.; Rachlew-Kallne, E.; Stromholm, C.; Larsson, J.; Persson, A.; Zerne, R. *Chem. Phys. Lett.* **1993**, *215*, 173.
(27) Chupka, W. A.; Lifshitz, C. *J. Chem. Phys.* **1968**, *48*, 1109.
(28) Klippenstein, S. J.; Harding, L. B. *J. Phys. Chem. A* **1999**, *103*, 9388
(29) Hessler, J.; P.; Ogren, P. J. *J. Phys. Chem. A* **1996**, *100*, 984
(30) Slagle, I. R.; Gutman, D.; Davies, J. W.; Pilling, M. J. *J. Chem. Phys.* **1988**, *92*, 2455.